

Miniature atomic magnetometer integrated with flux concentrators

W. Clark Griffith,^{1,a)} Ricardo Jimenez-Martinez,^{1,b)} Vishal Shah,² Svenja Knappe,¹ and John Kitching¹

¹Time and Frequency Division, National Institute of Standards and Technology, Boulder, Colorado 80305, USA

²Department of Physics, Princeton University, Princeton, New Jersey 08544, USA

(Received 17 November 2008; accepted 4 December 2008; published online 14 January 2009)

High permeability magnetic flux concentrators are used to enhance the sensitivity of an atomic magnetometer operating in the spin-exchange relaxation-free regime. The magnetometer uses a millimeter scale ^{87}Rb vapor cell and either mu-metal or Mn-Zn ferrite flux concentrators. The measured sensitivity gives excellent agreement with calculations of thermal noise from the concentrator material. The mu-metal concentrators allow a sensitivity of $50 \text{ fT Hz}^{-1/2}$, limited by thermal current magnetic noise. The ferrite concentrators are limited by thermal magnetization noise at low frequencies, and reach a sensitivity of $10 \text{ fT Hz}^{-1/2}$ for frequencies above 125 Hz. © 2009 American Institute of Physics. [DOI: 10.1063/1.3056152]

Operating in the spin-exchange relaxation-free (SERF) regime has allowed alkali atomic magnetometers¹ to achieve subfemtotesla sensitivities.^{2,3} In this technique, magnetic resonance broadening due to alkali-alkali spin-exchange collisions is eliminated by operation at low magnetic fields and high alkali density,⁴ such that the rate of spin-exchange collisions is much greater than the Larmor spin precession frequency. Taking advantage of the SERF regime, we recently demonstrated a miniature SERF magnetometer⁵ using a microfabricated, millimeter scale atomic vapor cell that achieved a sensitivity of $65 \text{ fT Hz}^{-1/2}$ at zero magnetic field. This can be compared to a previous chip-scale atomic magnetometer⁶ with a sensitivity of $5 \text{ pT Hz}^{-1/2}$ operating outside the SERF regime. The miniature SERF magnetometer is competitive with the sensitivity of high T_c superconducting quantum interference device (SQUID) magnetometers, and another order of magnitude improvement might provide a noncryogenic, potentially low power alternative to low T_c SQUIDS in certain applications.

In this work we look to enhance the sensitivity of our SERF magnetometer by adding high permeability flux concentrators that amplify the magnetic field inside the vapor cell. Flux concentrators have previously been used to improve the sensitivity of a wide variety of magnetic field sensor technologies, including Hall sensors,⁷ magnetoresistive sensors,⁸ and SQUIDS.⁹ The field concentration factor increases as the separation between the ends of the concentrators is reduced, which makes their use ideally suited for microfabricated vapor cells. The concentrators increase the overall footprint of the sensor, but the device retains the advantages of the lower light and heating power requirements of the chip-scale sensor. The concentrators also introduce potential nonlinearity and hysteresis effects, but these issues can essentially be avoided by staying within the SERF low magnetic field limit. In our case the SERF field limit is about 300 nT, but the addition of flux concentrators reduces the usable field range by $1/G_c$, where G_c is the concentration factor.

The basic magnetometer operation is the same as is described in Ref. 5, and an overview of the experimental setup is shown in Fig. 1(b). A microfabricated vapor cell¹⁰ containing ^{87}Rb atoms and 2 amagat of N_2 buffer gas is formed in a $1 \times 1 \times 1 \text{ mm}^3$ cavity in a silicon wafer with pyrex windows anodically bonded to the front and back. The cell is heated to $160 \text{ }^\circ\text{C}$ by running electrical current through a $50 \text{ } \Omega$ chip resistor mounted on the exterior of the cell. Magnetic fields due to the heater current are mitigated by applying alternating current at 355 kHz. The cell is mounted inside a three layer mu-metal magnetic shield in order to operate near zero magnetic field and to screen out environmental magnetic noise.

A single circularly polarized light beam from a vertical-cavity surface-emitting laser (VCSEL) operating at 795 nm is used to optically pump and probe the ^{87}Rb atoms. The magnetometer is sensitive to magnetic fields transverse to the light propagation direction. At zero magnetic field, efficient optical pumping occurs and the light transmission increases.

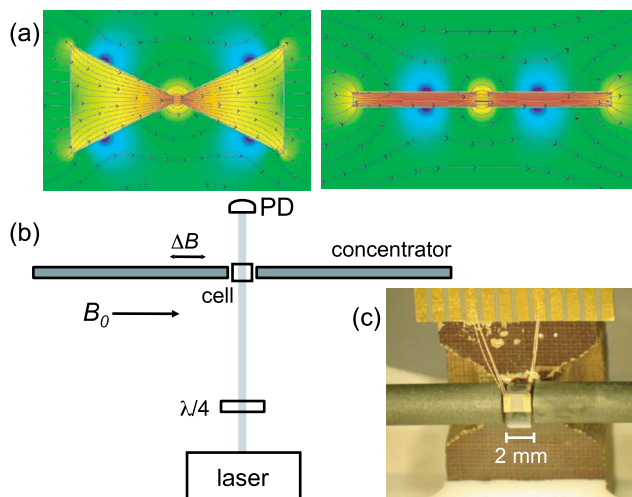


FIG. 1. (Color online) (a) Numerical calculation of the effect on flux lines and field density (false color) by triangular and rod shaped concentrators in a uniform external magnetic field. (b) Basic experimental setup. (c) Photograph of the vapor cell and the tips of the ferrite rod concentrators. The chip resistor used for heating the cell is visible on the front face.

^{a)}Electronic mail: clark.griffith@nist.gov.

^{b)}Also at University of Colorado, Boulder, CO.

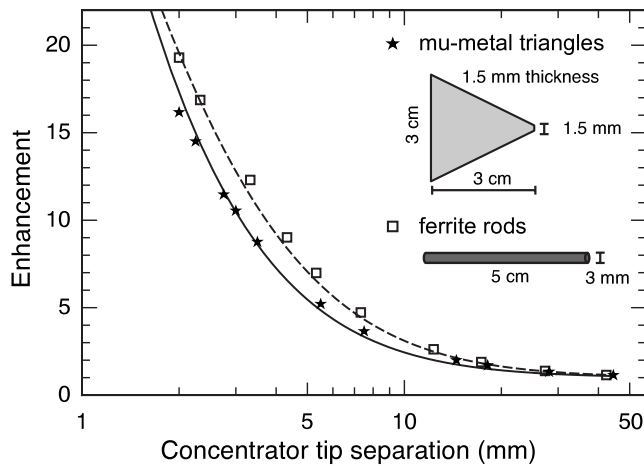


FIG. 2. Enhancement factor of a uniform externally applied magnetic field as the concentrators are moved closer to the cell. The data points give the measured enhancement, and the lines give the results of a finite element simulation for the mu-metal triangle (solid) and ferrite rod (dashed) concentrators.

For a nonzero transverse magnetic field (B_0) any optically pumped atoms quickly precess about the field so that no net polarization builds up, and the light transmission decreases. An additional modulated field at 1.5 kHz is applied parallel to B_0 , and lock-in detection is used to generate a dispersive signal as a function of the applied field. The magnetic field sensitivity is determined by setting B_0 to zero, and the noise spectral density of the lock-in signal is measured.

The transverse magnetic field is amplified inside the vapor cell by the addition of flux concentrators around the cell. Two types of concentrators were tested: flat mu-metal triangles ($\mu_r=3 \times 10^4$) and ferrite rods (high permeability Mn-Zn, $\mu_r=6 \times 10^3$).¹¹ A photograph of the ends of the ferrite concentrators around the vapor cell is shown in Fig. 1(c). Figure 2 shows the dimensions of the concentrators, along with the measured enhancement of a uniform external field compared to a finite element analysis calculation (lines) as the distance between the concentrators is varied. The minimum separation of the concentrators is limited to 2 mm by the external dimensions of the vapor cell.

The magnetic field sensitivity without concentrators was about $150 \text{ fT Hz}^{-1/2}$. This is about a factor of 2 worse than in Ref. 5 mainly due to differences in the vapor cell used in that work, which had a more favorable buffer gas pressure (3 amagat) and a larger cell cavity ($3 \times 2 \times 1 \text{ mm}^3$). Figure 3 shows the magnetic field sensitivity from noise density measurements at 40 and 150 Hz as the flux concentrators are moved closer to the cell. We expect that the sensitivity should improve by an amount equal to the enhancement factor shown in Fig. 2 up to the point where magnetic noise limits the sensitivity. Magnetic noise might originate from the concentrators themselves, or from other sources such as the magnetic shield material, current fluctuations in the field coils, or imperfectly shielded external noise.

In the case of the mu-metal concentrators, the sensitivity is limited to about $50 \text{ fT Hz}^{-1/2}$, whereas the ferrite concentrators reach a sensitivity of $15 \text{ fT Hz}^{-1/2}$ at 40 Hz and $10 \text{ fT Hz}^{-1/2}$ at 150 Hz. The sensitivity with the ferrite concentrators shows some excess magnetic noise at 40 Hz, but essentially follows the expected enhancement (red line) at 150 Hz. Figure 4 shows the noise spectral density converted

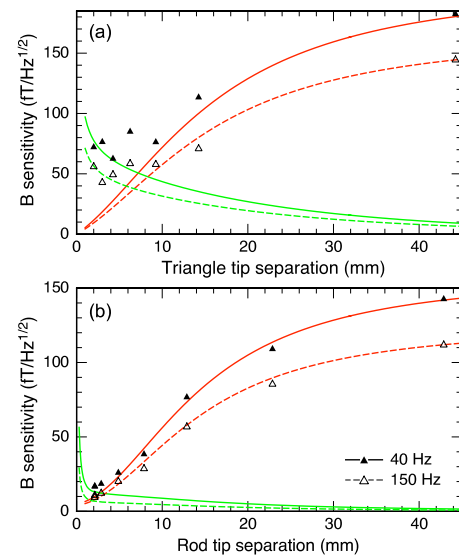


FIG. 3. (Color online) Magnetic field sensitivity vs flux concentrator tip separation for (a) the mu-metal triangle concentrators and (b) ferrite rod concentrators. The sensitivity is given for a noise density measurement at 40 Hz (solid points and lines) and 150 Hz (open points and dashed lines). The red lines indicate the sensitivity that would result if the unconcentrated sensitivity improved by the enhancement factors shown in Fig. 2, and the green lines show an estimate of the sensitivity limit due to thermal magnetic noise created by the flux concentrators.

into magnetic field units for the two types of concentrators at their most sensitive positions.

Thermal magnetic noise originating from the flux concentrator material can be estimated via fluctuation dissipation theorem methods.^{12,13} Following a numerical calculation approach similar to that described in Ref. 13, Appendix A, we use finite element analysis software to estimate the power loss P in the concentrators due to a hypothetical excitation coil located at the center of the vapor cell. The magnetic field noise at the location of the coil is then given by

$$\delta B = \frac{\sqrt{4kT}\sqrt{2P}}{NAI\omega}, \quad (1)$$

where the coil is assumed to have N turns, area A , and oscillating current I . The dissipative power loss has contributions from eddy current loss associated with Johnson noise cur-

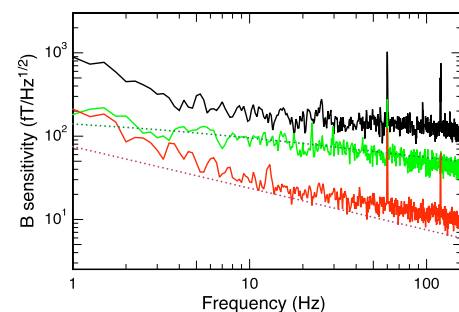


FIG. 4. (Color online) Noise density of the lock-in signal converted to magnetic field units for the sensor without flux concentrators (black), with the mu-metal triangle concentrators (green), and with the ferrite rod concentrators (red). The dotted green line shows an estimate of the thermal current noise due to the mu-metal concentrators and the dotted red line shows an estimate of the thermal magnetization noise due to the ferrite concentrators ($75 \text{ fT f}^{-1/2}$).

rents, and hysteresis loss associated with magnetic domain fluctuations:

$$P_{\text{eddy}} = \int_V \frac{1}{2} \sigma E^2 dV, \quad \text{and} \quad P_{\text{hyst}} = \int_V \frac{1}{2} \omega \mu'' H^2 dV, \quad (2)$$

where σ is the electrical conductivity, μ'' is the imaginary part of the complex permeability $\mu = \mu' - i\mu''$, E and H are the amplitudes of the electric and magnetic fields induced by the excitation coil, and the integration is carried out over the volume of the concentrators.

Johnson current noise generally has a flat spectrum at low frequencies until it begins to fall off at higher frequencies due to shielding effects, whereas magnetization noise has a $f^{-1/2}$ dependence.³ The noise in the mu-metal concentrators above 0.3 Hz is dominated by the Johnson current noise due to its relatively high electrical conductivity ($\sigma = 1.6 \times 10^6 \Omega^{-1} \text{m}^{-1}$, $\mu''/\mu_0 \approx 10^3$).³ The ferrite noise is dominated by thermal magnetization fluctuations and has negligible Johnson current noise ($\sigma = 0.2 \Omega^{-1} \text{m}^{-1}$, $\mu''/\mu_0 \approx 26$).¹⁴

As an example, with the ferrite rod concentrators at a 2 mm separation, our numerical calculation gives a noise estimate of 1.4 pT Hz^{-1/2} at 1 Hz at the center of the vapor cell. Since we are interested in our sensitivity in relation to the unconcentrated external field, the noise estimate is then divided by the flux concentration factor of 19, resulting in a 75 fT Hz^{-1/2} limit on the magnetometer sensitivity. Thermal magnetic noise limits of this type are displayed in Fig. 3 (green lines) and Fig. 4 (dotted lines). The excellent agreement between the noise estimates and the measured magnetic sensitivity spectrum shown in Fig. 4 strongly suggests that thermal current noise limits the sensitivity when the mu-metal concentrators are used, and thermal magnetization noise limits the sensitivity at low frequencies when the ferrite concentrators are used.

The low frequency sensitivity with the ferrite concentrators could potentially be improved by use of a material with a lower loss factor, $\mu''\mu_0/\mu'^2$. The thermal concentrator noise can also generally be mitigated by measuring at higher frequencies. With the ferrite concentrators the sensitivity reaches 10 fT Hz^{-1/2} at about 125 Hz, above which the sensitivity is limited by the unconcentrated sensitivity. The unconcentrated sensitivity might be improved with a better optimized buffer gas pressure cell, and by performing closer to the photon shot noise limit, which is a factor of 5 lower than the present noise level. The intrinsic bandwidth of the magnetometer is about 1 kHz, determined by the relaxation rate of the spin resonance, but the effective bandwidth of the magnetometer was 260 Hz in these measurements, set by the lock-in detector time constant (0.3 ms) and filter roll-off (24 dB/octave).

An additional advantage of the use of flux concentrators is that they allow sensitivity improvement while maintaining the signal bandwidth of the unconcentrated sensor. This is in contrast with the approach of improving sensitivity by reduc-

ing the magnetic resonance linewidth, which generally reduces the bandwidth of the sensor. For example, the extremely high sensitivities of the SERF magnetometers in Refs. 2 and 3 are achieved through very narrow magnetic resonance linewidths, resulting in relatively low bandwidths of 20 and 10 Hz, respectively. Integrating flux concentrators with a larger linewidth sensor is potentially advantageous in applications requiring both high sensitivity and bandwidth.

In summary, we have examined the use of mu-metal and ferrite flux concentrators to improve the sensitivity of a miniature SERF atomic magnetometer. The concentrators enhance the magnetic field inside the vapor cell by up to a factor of 19 when moved to their closest positions, but also contribute magnetic noise that matches very well with numerical modeling of the Johnson current noise and thermal magnetization noise in the mu-metal and ferrite, respectively. The Johnson current noise limits the mu-metal concentrator sensitivity to about 50 fT Hz^{-1/2}, and the thermal magnetization noise limits the ferrite concentrator sensitivity to 75 fT Hz^{-1/2} at low frequencies, reaching a sensitivity of 10 fT Hz^{-1/2} for the frequency range of 125–200 Hz. The flux concentrators somewhat increase the sensor size, but we still retain the advantages of a potentially low power, highly sensitive sensor using a single VCSEL light source.

The authors thank S. Schima for help in preparing the cell assembly, S.-K. Lee for help with the noise estimations, H. B. Dang for information on ferrite permeability measurements, and Y.-J. Wang and J. Preusser for valuable discussions. This work was supported by the Strategic Environmental Research and Development Program (SERDP).

¹D. Budker and M. Romalis, *Nat. Phys.* **3**, 227 (2007).

²I. K. Kominis, T. W. Kornack, J. C. Allred, and M. V. Romalis, *Nature (London)* **422**, 596 (2003).

³T. W. Kornack, S. J. Smullin, S. K. Lee, and M. V. Romalis, *Appl. Phys. Lett.* **90**, 223501 (2007).

⁴W. Happer and H. Tang, *Phys. Rev. Lett.* **31**, 273 (1973).

⁵V. Shah, S. Knappe, P. D. D. Schwindt, and J. Kitching, *Nat. Photonics* **1**, 649 (2007).

⁶P. D. D. Schwindt, B. Lindseth, S. Knappe, V. Shah, J. Kitching, and L. A. Liew, *Appl. Phys. Lett.* **90**, 081102 (2007).

⁷P. Leroy, C. Coillot, A. F. Roux, and G. M. Chanteur, *IEEE Sens. J.* **6**, 707 (2006).

⁸A. S. Edelstein, G. A. Fischer, M. Pedersen, E. R. Nowak, S. F. Cheng, and C. A. Nordman, *J. Appl. Phys.* **99**, 08B317 (2006).

⁹S. I. Bondarenko, A. A. Shablo, P. P. Pavlov, and S. S. Perepelkin, *Physica C* **372**, 158 (2002).

¹⁰S. Knappe, V. Gerginov, P. D. D. Schwindt, V. Shah, H. G. Robinson, L. Hollberg, and J. Kitching, *Opt. Lett.* **30**, 2351 (2005).

¹¹MN60 from Ceramic Magnetics Inc. This information is provided for completeness of technical description only, and implies no endorsement by NIST. Similar products from other manufacturers may work as well or better.

¹²H. B. Callen and T. A. Welton, *Phys. Rev.* **83**, 34 (1951).

¹³S. K. Lee and M. V. Romalis, *J. Appl. Phys.* **103**, 084904 (2008).

¹⁴The manufacturer provided data sheet gives $\mu''/\mu_0 \approx 45$ at 15 kHz. Measurements by Dang and Romalis indicate that $\mu''/\mu_0 \approx 26$ at frequencies below 200 Hz (private communication).